Coherent spin relaxation in molecular magnets

V.I. Yukalov[1], V.K. Henner[2,3], and P.V. Kharebov[2]

[1]*Bogolubov Laboratory of Theoretical Physics,*
Joint Institute for Nuclear Research, Dubna 141980, Russia

[2]*Perm State University, Perm 614000, Russia*

[3]*University of Louisville, Louisville 40292, KY, USA*

Abstract

Numerical modelling of coherent spin relaxation in nanomagnets, formed by magnetic molecules of high spins, is accomplished. Such a coherent spin dynamics can be realized in the presence of a resonant electric circuit coupled to the magnet. Computer simulations for a system of a large number of interacting spins is an efficient tool for studying the microscopic properties of such systems. Coherent spin relaxation is an ultrafast process, with the relaxation time that can be an order shorter than the transverse spin dephasing time. The influence of different system parameters on the relaxation process is analysed. The role of the sample geometry on the spin relaxation is investigated.

PACS: 76.20.+q, 75.30.Gw, 75.45.+j, 75.50.Xx, 76.90.+d

1 Introduction

A polarized magnet placed in an external magnetic field, whose direction is opposite to the sample magnetization, comprises a strongly nonequilibrium system. The relaxation of spins to their equilibrium position can occur in different ways. The simplest process is the slow relaxation during the time T_1 caused by the spin-lattice coupling [1], when the total magnetization tends to zero. This is an incoherent process, since T_1 is usually much longer than the spin dephasing time T_2. A straightforward way to make the spin relaxation coherent would be by imposing a strong transverse field simultaneously driving all spins, which would represent the process of *free induction* [1], lasting for the time T_2. This, however, is a rather trivial process, when spins are practically independent of each other.

A more elaborate situation arises if the magnet is inserted into a magnetic coil of a resonant electric circuit. Then the magnetic field, induced by the coil, provides an efficient feedback mechanism organizing the coherent motion of spins [2]. It is possible to realize six different regimes of coherent spin relaxation in a polarized sample coupled to a resonant circuit: *Collective induction, maser generation, pure superradiance, triggered superradiance, pulsing superradiance*, and *punctuated superradiance*. A detailed description of these regimes is given in the review articles [3–5].

Collective induction and maser generation with spins were realized in a number of experiments [6–9]. Pure spin superradiance was, first, observed in Dubna [10,11] and later confirmed by the groups in St. Petersburg [12,13] and Bonn [14]. Pulsing superradiance was demonstrated by experiments in Zürich [15,16]. The regime of punctuated superradiance was suggested in Ref. [17] and, to our knowledge, has not yet been realized experimentally. A comprehensive survey of experiments can be found in Refs. [4,5,18].

It is necessary to emphasize the principal role of the resonant electric circuit, coupled to the spin sample, for realizing the regimes of spin superradiance. This makes the fundamental difference between the spin superradiance and the atomic superradiance [19]. The latter can be achieved in a resonatorless system [19–21], though a resonant cavity can enhance the effect [22,23]. Contrary to this, the spin superradiance, occurring in the radiofrequency range, cannot be realized without a resonator, which is due to the destructive role of the dipole spin interactions and to the absence of the feedback mechanism collectivizing the spin motion. This basic difference was emphasized in Ref. [19] and thoroughly explained in Refs. [5,24,25]. One should also distinguish between coherent transient effects, caused by intense alternating external fields, and having much in common for optical atomic systems [20,21], gamma radiation [26–29], as well as for spin samples [30–32], and superradiant phenomena, when the *self-organization* of coherence is the basic origin of the arising superradiance [25,33,34].

Here we concentrate our attention on the superradiant regime of spin motion, which requires the presence of the resonant electric circuit, providing the feedback mechanism for the collective self-organization of spin motion. The regimes of free induction, collective induction, and triggered spin superradiance could be considered in the frame of the phenomenological Bloch equations supplemented by the Kirchhoff equation for the circuit [35–38]. These phenomenological equations, however, are not applicable for describing pure spin superradiance, when the coherent motion of spins develops in a self-organized way from initially chaotic spin fluctuations. The complete theory, based on the microscopic spin Hamiltonian, and describing all regimes of spin relaxation has been developed in Refs. [18,25,33,34,39] and expounded in detail in the review articles [4,5]. This theory is in good agreement with

experiment [4,5] as well as with numerical computer simulations [40–42] accomplished for nuclear or electron spins one half, $S = 1/2$.

There also exists a wide class of paramagnetic materials formed by magnetic molecules [43], whose effective ground-state spins can reach rather high values of $S \sim 10$. These molecules compose molecular magnets whose properties are described at length in Refs. [5,18,44,45]. For example, the molecules Mn_{12} and Fe_8 possess the spin $S = 10$. The magnetic cluster compound $Mn_6O_4Br_4(Et_2dbm)_6$ has the total spin $S = 12$ [46]. And the magnetic molecule $Cr(CNMnL)_6(ClO_4)_9$, where L stands for a neutral pentadentate ligand, displays the effective spin $S = 27/2$ [45].

Molecular magnets, formed by high-spin magnetic molecules, exhibit a rather strong magnetic anisotropy and a gigantic relaxation time of their magnetization, which reaches about two months in zero magnetic field at low temperature [5,18,44,45]. The magnetization relaxation is mainly due to the phonon-assisted mechanism caused by spin-phonon interactions [47,48]. The fast superradiant-type relaxation of magnetization is theoretically possible for molecular magnets, provided they are placed in a sufficiently strong external magnetic field and necessarily coupled to a resonant circuit [5,18,25,49].

The main points, distinguishing the relaxation in magnetic molecules, studied earlier [44,45,50–57], from the process to be investigated in the present paper, are as follows.

First of all, the usually studied spin relaxation in magnetic molecules is the process of quantum tunneling occurring in individual molecules [50–57]. Contrary to this, we shall be interested in coherent, principally collective effects, due to strong correlations between many molecules, which is caused by the resonator feedback field.

Quantum tunneling in separate molecules is known to be phonon assisted, with an essential phonon influence on the relaxation process [47,48,58]. But in the case of spins strongly correlated through the resonant feedback field, spin-phonon interactions are not as important, the basic dynamics being governed by the resonator feedback field.

The single-molecule spin relaxation is not connected with a fixed particular frequency [59], because of a sufficiently strong magnetic anisotropy and a varying external magnetic field [5,19,24,25]. While to realize the collective coherent spin relaxation necessary requires the situation close to resonance between the Zeeman frequency and the resonator natural frequency.

Magnetic avalanches are usually accomplished by sweeping the longitudinal magnetic field with a rather slow sweeping rate. A typical field sweeping rate used in experiments [50–55] is about 0.1 T/s. In our case, we consider a fixed external magnetic field, with a well defined Zeeman frequency.

The avalanche time of the magnetic moment in magnetic molecules is between 10^{-3} s and 1 s [50–57,59]. This is rather slow process, as compared to the coherent spin relaxation, which is an ultrafast process, with characteristic relaxation times about $10^{-10} - 10^{-13}$ s [5,18,24,25,49].

The peculiarities of the fast superradiant-type spin relaxation in molecular magnets can be successfully analyzed by means of computer modelling, which, to our knowledge, has not yet been accomplished. This approach provides a very efficient tool for studying the microscopic properties of spin system. And it is the aim of the present paper to describe the results of computer simulations for analyzing the features of the fast coherent relaxation of molecular spins, typical of the high-spin molecular magnets.

The outline of the paper is as follows. In Sec. II, we present the main definitions and

equations to be employed in our computer modelling. In Sec. III, the results for a bulk sample are analyzed. Since the dipolar spin interactions are anisotropic, it is interesting to study the related anisotropic geometric effects for different shapes of the magnetic samples. These geometric effects are investigated for a chain of molecular spins oriented either along the external magnetic field or perpendicular to it and for spin planes, with the external magnetic field being either perpendicular to it or lying in that plane. Section IV contains conclusions.

2   Basic Definitions and Equations

We consider a spin sample characterized by the molecular spin vectors $\mathbf{S}_j = \{S_j^x, S_j^y, S_j^z\}$ associated with the lattice sites enumerated by the index $j = 1, 2, \ldots, N$. An external magnetic field is directed along the z-axis,

$$\mathbf{B}_0 = B_0 \, \mathbf{e}_z \ . \tag{1}$$

This defines the Zeeman frequency

$$\omega_0 \equiv -\frac{\mu_0}{\hbar} \, B_0 = \frac{2}{\hbar} \, \mu_B \, B_0 \ , \tag{2}$$

in which $\mu_0 = -2\mu_B$ is the electron magnetic moment, with μ_B being the Bohr magneton. In general, similarly to the magnetic-resonance setup, there can exist the transverse magnetic field, directed along the x-axis,

$$\mathbf{B}_1 = B_1 \mathbf{e}_x \ , \qquad B_1 = h_0 + h_1 \cos \omega t \ , \tag{3}$$

and consisting of a constant field h_0 and an alternating field $h_1 \cos \omega t$.

Molecular magnets possess the single-site magnetic anisotropy characterized by the anisotropy parameter D, which defines the anisotropy frequency

$$\omega_D \equiv (2S - 1) \, \frac{D}{\hbar} \ , \tag{4}$$

where S is the molecular spin. The magnetic anisotropy exists for high spins, playing an important role, while for $S = 1/2$ it disappears, according to Eq. (4).

Spins interact with each other through the dipolar forces characterized by the dipolar tensor

$$D_{ij}^{\alpha\beta} \equiv \frac{\mu_0^2}{r_{ij}^3} \, \left(\delta_{\alpha\beta} - 3n_{ij}^\alpha \, n_{ij}^\beta \right) \ , \tag{5}$$

in which

$$r_{ij} \equiv |\mathbf{r}_{ij}| \ , \qquad \mathbf{n}_{ij} \equiv \frac{\mathbf{r}_{ij}}{r_{ij}} \ , \qquad \mathbf{r}_{ij} \equiv \mathbf{r}_i - \mathbf{r}_j \ .$$

For what follows, it is convenient to introduce the dipolar coefficients

$$a_{ij} \equiv D_{ij}^{zz} \ , \qquad b_{ij} \equiv \frac{1}{4} \left(D_{ij}^{xx} - D_{ij}^{yy} - 2iD_{ij}^{xy} \right) \qquad c_{ij} \equiv \frac{1}{2} \left(D_{ij}^{xx} - iD_{ij}^{yz} \right) \ , \tag{6}$$

having dimensions of energy.

The spin sample is inserted into a magnetic coil of an electric circuit characterized by the circuit damping γ and the circuit natural frequency ω. Moving spins generate electric current in the coil, which, in turn, produces the feedback magnetic field $\mathbf{H}$ acting on the spins. The generated electric current is described by the Kirchhoff equation. Choosing the coil axis along the x-axis, so that $\mathbf{H} = H\mathbf{e}_x$, the Kirchhoff equation can be rewritten [33,34] as the equation for the feedback magnetic field H,

$$\frac{dH}{dt} + 2\gamma H + \omega^2 \int_0^t H(t') \, dt' = -4\pi\eta \frac{dm_x}{dt} \; , \tag{7}$$

where the effective electromotive force in the right-hand side of Eq. (7) is produced by moving spins, with the average magnetization

$$m_x = \frac{\mu_0}{V} \sum_{j=1}^N < S_j^x > \; , \tag{8}$$

V being the sample volume. The filling factor η in the right-hand side of Eq. (7) is approximately equal to $\eta = V/V_c$, where V_c is the coil volume. For what follows, without the loss of generality, we may assume the dense filling, with $\eta = 1$. Instead of Eq. (7), we can use the equivalent differential equation

$$\frac{d^2 H}{dt^2} + 2\gamma \frac{dH}{dt} + \omega^2 H = -4\pi \frac{d^2 m_x}{dt^2} \; , \tag{9}$$

in which we set $\eta = 1$.

All possible attenuation mechanisms have been carefully described in Ref. [25]. Those that influence the spin motion are as follows. The longitudinal attenuation

$$\Gamma_1 = \gamma_1 + \gamma_1^* \tag{10}$$

is the sum of the spin-lattice attenuation γ_1, caused by spin-phonon interactions, and of the polarization pump rate γ_1^*, due to a stationary nonresonant pump, if any. The total transverse attenuation is

$$\Gamma_2 = \gamma_2 \left(1 - s^2\right) + \gamma_2^* \; . \tag{11}$$

This includes the homogeneous broadening γ_2, renormalized by the factor $(1 - s^2)$, appearing in the case of strongly polarized spin systems [1,25], with s being the average spin polarization reduced to the number of spins N and to the spin value S. The last term γ_2^* is the static inhomogeneous broadening.

In order to represent the equations of spin motion in a compact form, it is convenient to introduce the ladder spin components

$$S_j^- \equiv S_j^x - iS_j^y \; , \qquad S_j^+ \equiv S_j^x + iS_j^y \; . \tag{12}$$

Also, we shall use the following notation:

$$\xi_i^0 \equiv \frac{1}{\hbar} \sum_{j(\neq i)} \left(a_{ij}S_j^z + c_{ij}^* S_j^- + c_{ij}S_j^+\right) \; ,$$

$$\xi_i \equiv \frac{1}{\hbar} \sum_{j(\neq i)} \left(2c_{ij}S_j^z - \frac{1}{2} a_{ij}S_j^- + 2b_{ij}S_j^+ \right) . \tag{13}$$

The effective force, acting on the j-spin, can be written as

$$f_j \equiv -\frac{i}{\hbar} \mu_0(B_1 + H) + \xi_j . \tag{14}$$

The derivation of equations of motion for the spin variables S_j^-, S_j^+, and S_j^z has been described in great detail in Refs. [4,5,25]. The resulting equation for S_j^- reads as

$$\frac{dS_j^-}{dt} = -i \left(\omega_0 + \xi_j^0 - i\Gamma_2 \right) S_j^- + f_j S_j^z + i \frac{\omega_D}{S} S_j^z S_j^- . \tag{15}$$

The equation for S_j^+ is conjugate to Eq. (15). And the equation for S_j^z is

$$\frac{dS_j^z}{dt} = -\frac{1}{2} \left(f_j^+ S_j^- + S_j^+ f_j \right) - \Gamma_1 \left(S_j^z - \zeta \right) , \tag{16}$$

where ζ is the stationary spin polarization. From Eqs. (15) and (16), with notation (12), one can always return to the evolution equations for S_j^x, S_j^y, and S_j^z.

In numerical simulations, one treats the spins $\mathbf{S}_j$ as classical vectors [40–42]. It is convenient to work with the reduced quantities characterizing the reduced transverse spin variable

$$u \equiv \frac{1}{SN} \sum_{j=1}^N S_j^- \tag{17}$$

and the reduced longitudinal spin variable

$$s \equiv \frac{1}{SN} \sum_{j=1}^N S_j^z . \tag{18}$$

The spin variables (17) and (18) characterize the collective properties of a large number of magnetic molecules composing the molecular magnet. The time evolution of these variables is prescribed by the equations of motion (15) and (16). This picture of collective spin motion is a generalization of the evolution equations for a single magnetic molecule. The study of collective coherent effects is the main aim of the present paper.

In our numerical simulations, we solve the spin evolution equations (15) and (16) for a finite number of spins N. The resonator feedback field is given by Eq. (9), with the initial conditions

$$H(0) = 0 , \qquad \dot{H}(0) = 0 , \tag{19}$$

where the overdot implies the time derivative of H. The spin variables S_j^α at the initial time are distributed randomly over the sample, so that to obtain a prescribed value $s(0)$ of the spin polarization (18), while variable (17), for sufficiently high initial spin polarization, being negligible,

$$s(0) = s_0 , \qquad u(0) = 0 . \tag{20}$$

The external magnetic field (1), with $B_0 > 0$, is aligned with $\mathbf{e}_z$. For the initial spin polarization $s_0 > 0$, the magnetic moment of the molecular sample

$$\mathbf{M}(0) = NS\mu_0 s_0 \mathbf{e}_z = -2NS\mu_B s_0 \mathbf{e}_z$$

is opposed to $\mathbf{e}_z$. That is, the considered molecular magnet is prepared in a strongly nonequilibrium initial state, from which it relaxes to a stationary state.

3 Results of Computer Simulation

First, we consider the coherent spin relaxation in bulk samples, where spins are located in lattice sites of a cubic lattice. Computer simulations are accomplished for $N = 125$ spins. For larger values of N, the results are qualitatively similar. The periodic boundary conditions have been imposed. Since our aim is to study the self-organized process, we set zero the transverse field $B_1 = 0$. We assume that the spin sample is without defects, so that the inhomogeneous broadening is negligible, $\gamma_2^* = 0$. For low temperatures, the spin-lattice interaction in molecular magnets is very weak, with the longitudinal relaxation time T_1 reaching months (see review articles [5,18,44,45]), because of which the attenuation parameter Γ_1 plays no role, and we can set $\Gamma_1 = 0$. It is convenient to deal with dimensionless quantities measuring all frequencies in units of γ_2, so that we set $\gamma_2 = 1$. And we shall measure time in units of γ_2^{-1}, that is, in units of T_2.

First and foremost, we have to stress the necessity of the resonant circuit. When the latter is absent, there is no fast relaxation at all. Then there could exist only the very slow polarization decay during the time T_2, which is caused by spin interactions. The same slow relaxation happens if there is a circuit, but there is no resonance between its natural frequency ω and the Zeeman frequency ω_0. Therefore, in what follows, we always set $\omega = \omega_0$. This resonance condition is necessary, though not sufficient. To realize an effective spin reversal, it is important that ω_0 be much larger than the anisotropy frequency (4). The condition $\omega_0 \gg \omega_D$ ensures that the anisotropy does not induce an effective detuning from the resonance [5,18,24,25].

Figure 1 illustrates how the spin reversal depends on the value of the Zeeman frequency ω_0. The larger the latter, the more pronounced is the spin reversal.

The resonator damping γ defines the resonator ringing time $\tau \equiv 1/\gamma$, during which the magnetic sample effectively interacts with the resonator. The relation between the resonator ringing time τ and the transverse relaxation time T_2 essentially influences the spin reversal. When $\tau = T_2$, then there is a permanent exchange of energy between the spin sample and the resonator, so that the spin polarization oscillates around zero. When $\tau = 0.1\, T_2$, there occurs a well pronounced reversal, hence the value $\gamma = 10$ is optimal for the latter. And if $\tau = 0.02\, T_2$, then the effective interaction time between the sample and resonator is too short to realize a good reversal of polarization. The corresponding three qualitatively different cases ate shown in Fig. 2.

The magnitude of spin reversal also depends on the initial polarization. The larger the initial value s_0, the stronger the spin reversal, which is illustrated in Fig. 3.

Magnetic anisotropy is an obstacle for the coherent spin relaxation. The larger the value of ω_D, the smaller the spin reversal, as is demonstrated in Fig. 4.

Dipole spin interactions is also a factor suppressing spin coherence. This is illustrated by Fig. 5, where the behavior of spin polarization for the case with dipole interactions is compared with that one, for which the dipole interactions are switched off by setting $D_{ij}^{\alpha\beta} = 0$.

It is interesting that switching off the dipole interactions yields the figures that are very close to those obtained by the reduction of spin from $S = 10$ to $S = 1/2$. Thus the dashed line in Fig. 5, where $\gamma = 10$, for $S = 10$ can be repeated not by setting the dipole tensor to zero but by reducing the spin to $S = 1/2$. In Fig. 6, we show the behavior of spin polarization for $S = 10$ and $S = 1/2$ for $\gamma = 1$. Again, switching off the dipole interactions

for $S = 10$ yields the dashed curve corresponding to $S = 1/2$ with dipole interactions.

Dipole interactions are anisotropic. Therefore, their influence on the relaxation process can be different for the samples of different shapes and of different orientations with respect to the external magnetic field and with respect to the resonator feedback field. To analyze these differences, we study the spin relaxation, under the same system parameters, but for different samples. We consider the chain of spins oriented either along the external magnetic field, i.e., along the z-axis, or along the feedback field, that is, along the x-axis. And we consider the plane of spins, oriented either in the $y-z$ plane or in the $x-y$ plane. The results of computer simulation for $N = 144$ spins are presented in Fig. 7. These results demonstrate that the maximally efficient spin reversal happens for the chain of spins directed along the x-axis. This looks quite understandable, since the x-axis is the axis of the direction of the resonator feedback field, which is the main source of the coherent spin motion.

4 Discussion

We have accomplished computer simulations of the coherent spin relaxation in molecular magnets with large spin. The investigation is based on the microscopic model taking into account realistic dipole spin interactions and the single-site magnetic anisotropy. The system is prepared in a strongly nonequilibrium state, with an external magnetic field opposite to the sample magnetization.

The principal point of our investigation is the presence of a resonator coupled to the sample. The later is inserted into a coil of an electric circuit, whose natural frequency is in resonance with the Zeeman frequency. Without the resonator, the coherent spin motion is impossible. It is the resonator feedback field, which collectivizes the spin motion, making it well correlated, hence, coherent.

To realize the coherent spin relaxation, the Zeeman frequency ω_0 has to be much larger than the anisotropy frequency ω_D. An efficient spin reversal requires that the initial spin polarization be sufficiently high, the higher, the better, The typical spin reversal time τ is an order smaller than the transverse dephasing time T_2, which translates into the relation $\gamma \sim 10\gamma_2$.

The role of dipole spin interactions, *in the presence of a resonator*, is twofold, making the spin dynamics in a sample coupled to a resonator rather different from that happening in a sample with no resonator feedback fields.

From one side, dipole interactions influence the spin motion by making the spin reversal less pronounced. For low spins, such as $S = 1/2$, dipole interactions are less important than for large spins $S = 10$. Emphasizing the decoherence influence of the dipolar interactions, we should keep in mind that our simulations are performed for a finite number of spins. The majority of our calculations are done for 125 spins. Because of the long range of the dipolar forces, increasing the number of spins strengthens the decohering influence of these forces. However, all qualitative results remain, as we have checked by varying the number of spins between 64 and 343. Also, presenting the results in dimensionless units, as we have done, when all frequencies and attenuation parameters are normalized by the dipolar interaction strength, makes the calculated curves for the average magnetization practically independent of the sample size. Increasing the number of interacting spins simply implies the renormalization of the dimensionless quantities and does not change their behavior represented in

dimensionless units.

At the same time, increasing the number N of spins strengthens the role of the resonator feedback field, which makes the process of spin coherentization faster, so that the relaxation time, due to the coherent spin motion, depends on the number of spins as $1/N$.

In this way, stronger dipole interactions, from one side, increase the transverse decoherence attenuation, but, from another side, they induce stronger coherence through the action of the resonator feedback field, making the coherent relaxation faster. These two opposite effects, to some extent, compensate each other. Therefore, the coherent spin dynamics, occurring in the presence of a resonator, qualitatively does not change much under the variation of spin number.

Our main concern in the present paper has been the study of spin dynamics for large spins. This is why we have done numerical simulations for $S = 10$. We have had no aim of studying the low-spin dynamics, such as that of spins one-half, since this dynamics has been considered earlier. It is only to note that the low-spin dynamics is rather different that we show its qualitative difference in one curve of Fig. 6.

It is worth mentioning that for large spins $S \geq 1$ it is feasible to consider spin transitions between different sublevels labelled by the z-projection number $m = -S, -S+1, \ldots, S-1, S$. A pair of sublevels can be treated as an effective two-level system [56,57]. Then to realize the coherent spin relaxation, one has to tune the resonant natural frequency to the transition frequency between the chosen two levels. For high nuclear spins, this procedure was realized experimentally [15,16]. Hence, in the same way it can be realized for molecular magnets.

It is important to stress that there are several principle physical differences between the experiments with nuclear spins, described in Refs. [15,16], and the situation considered in the present paper. In these experiments [15,16], the nuclei of ^{27}Al inside the ruby crystal were studied. *First* of all, the nuclei of ^{27}Al possess spins $I = 5/2$, which are not as large as we have considered here, dealing with $S = 10$. *Second*, in the case of ^{27}Al, an external resonant circuit was tuned to the central line $\{-1/2, 1/2\}$, with a fixed transition frequency $\omega_0 \sim 10^8$ Hz, thus, reducing the consideration to an effective two-level system with spin one-half, while here we always have dealt with the total spin $S = 10$, since we have considered the resonant circuit tuned to the transition between $-S$ and S. *Third*, as we have shown, for our high-spin case the influence of dipolar interactions is essential, while their role for an effective one-half spin system [15,16] is not of such importance. *Fourth*, contrary to the case of nuclear spins, having no single-site anisotropy, the molecular magnets, we have studied, exhibit quite strong magnetic anisotropy, fundamentally distorting spin dynamics and making it principally different as compared with the isotropic case of nuclear spins. *Fifth*, for strongly polarized spin materials, it is necessary to take account of the saturation effect making the total transverse attenuation depending on the polarization level [1,25], as in Eq. (11), while this effect does not play role for not so strong polarization [15,16]. *Sixth*, in experiments [15,16], pulsing spin dynamics was analyzed, when the inversion of spin polarization was permanently supported by constantly applied dynamic nuclear polarization with a rather high pumping rate, while we studied the pure coherent spin relaxation, when there is no permanent pumping. *Finally*, we have studied here the dependence of spin relaxation on the sample shape and orientation. Such geometric effects, to our knowledge, have not been investigated. These seven factors make the spin dynamics in our case and in the case of Refs. [15,16] principally different.

When studying the geometric effects related to the sample shape and its orientation,

differently oriented spin chains and planes have been considered. We have found that, under the same system parameters, including the number of spins, except the sample shape and orientation, the most efficient coherent spin relaxation, with the deepest spin reversal, happens for a chain of spins aligned with the direction of the resonator feedback field.

The main aim of the present paper has been to analyze the coherent spin relaxation under widely varying system parameters, in order to clarify the influence of different parameters on the coherent spin motion. This should help in choosing the optimal materials for realizing such a coherent spin motion. Nowadays, there are plenty of magnetic materials, with widely varying properties, which could be used for experimentally observing the described effects. The description of the properties of various molecular magnets can be found in the review articles [5,18,44,45].

As an example, we can mention the most often studied molecular magnets made of the molecules Mn_{12} or Fe_8, whose spins are $S = 10$. For these materials, $\omega_D \sim 10^{12}$ s^{-1}. At low temperatures, below the blocking temperature of about 1 K, the sample can be polarized, having a very long spin-lattice relaxation time $T_1 \sim 10^5 - 10^7$ s. Hence $\gamma_1 \equiv 1/T_1$ is practically negligible, $\gamma_1 \sim 10^{-7} - 10^{-5}$ s^{-1}. Dipole spin interactions in these materials are rather strong, with $\gamma_2 \sim 10^{10}$ s^{-1}. To realize the coherent spin relaxation, the external magnetic field B_0 is to be sufficiently strong, such that corresponding Zeeman frequency ω_0, being close to the resonator natural frequency ω, would be much larger than the anisotropy frequency ω_D. For the considered case of Mn_{12} or Fe_8, this requires the field $B_0 \sim 100$ T. This is a strong field, though which can experimentally be reached [60]. Fortunately, there are many other molecular magnets with a smaller anisotropy. For instance, in the case of nanomagnets formed by the molecules Mn_6, whose spin is $S = 12$, the magnetic anisotropy is much lower, with $\omega_D \sim 10^{10}$ s^{-1}. Therefore the required external magnetic field is only about $B_0 \sim 1$ T, which is the standard field used in laboratory.

The existence of the magnetic anisotropy typical of many molecular magnets, hinders the feasibility of the coherent spin relaxation. However, there are many magnetic materials with a small anisotropy, which should not disturb the coherent spin motion. In addition, the influence of the magnetic anisotropy can always be suppressed by a sufficiently strong external magnetic field. Fortunately, there exists in the world the possibility of creating very strong magnetic fields. Among available sources [60], we may mention those where the magnetic fields up to 45 T (USA) and even 600 T (Japan) can be reached.

In order to estimate the typical time of the coherent spin relaxation, we may notice that this time is an order smaller than T_2. The spin dephasing time in molecular magnets, such as Mn_{12} and Fe_8, is due to dipole interactions yielding $\gamma_2 \sim 10^{10}$ s^{-1}. Hence $T_2 \sim 10^{-10}$ s. This means that the typical time of the coherent spin relaxation in these materials is 10^{-11} s, which is an ultrafast process.

In conclusion, it is worthwhile to mention that for many magnetic molecules the influence of hyperfine interactions from nuclear spins could be important. These interactions result in the appearance of an additional line broadening, which can be included in the effective attenuation parameters, so that the existence of the hyperfine interactions can be taken into account by the appropriate definition of the effective attenuations, as has been done in Ref. [42]. At the same time, for many molecules, typical of the large family of magnetic molecules, such as Mn_{12} and Fe_8, the hyperfine interactions are of the order of 10^{-3} K, which are much weaker than the dipolar interactions, being of the order of 0.1 K (see details in

the review articles [5,18,44,45]). When the hyperfine interactions are two orders smaller than the dipolar interactions, the former, with a very good approximation, can be neglected. And if the former are comparable with the latter, this can be taken into account by the corresponding definition of the line broadening.

Acknowledgement

References

[1] A. Abraham and M. Goldman, *Nuclear Magnetism: Order and Disorder* (Clarendon, Oxford, 1982).

[2] N. Bloembergen and R.V. Pound, Phys. Rev. **95**, 8 (1954).

[3] V.I. Yukalov and E.P. Yukalova, Phys. Part. Nucl. **31**, 561 (2000).

[4] V.I. Yukalov in *Encyclopedia of Nuclear Magnetic Resonance*, edited by D.M. Grant and R.K. Harris (Wiley, Chichester, 2002), Vol. 9, p. 697.

[5] V.I. Yukalov and E.P. Yukalova, Phys. Part. Nucl. **35**, 348 (2004).

[6] G. Feher, J.P. Gordon, E. Buehler, E.A. Gere, and C.D. Thurmond, Phys. Rev. **109**, 221 (1958).

[7] A.E. Siegman, *Microwave Solid-State Masers*, (McGraw-Hill, New York 1964).

[8] V.M. Fain and Y.I. Khanin, *Quantum Electronics* (Pergamon, Oxford, 1969).

[9] A. Yoshimi, K. Asahi, K. Sakai, M. Tsuda, K. Yogo, H. Ogawa, T. Suzuki, and M. Nagakura, Phys. Lett. A **304**, 13 (2002).

[10] J.F. Kiselev, A.F. Prudkoglyad, A.S. Shumovsky, and V.I. Yukalov, Mod. Phys. Lett. B **1**, 409 (1988).

[11] Y.F. Kiselev, A.F. Prudkoglyad, A.S. Shumovsky, and V.I. Yukalov, J. Exp. Theor. Phys. **67**, 413 (1988).

[12] N.A. Bazhanov, D.S. Bulyanitsa, A.I. Kovalev, V.V. Polyakov, V.Y. Trautman, E.D. Trifonov, and A.V. Shvedchikov, Phys. Solid State **31**, 206 (1989).

[13] N.A. Bazhanov, D.S. Bulyanitsa, A.I. Zaitsev, A.I. Kovalev, V.A. Malyshev, and E.D. Trifonov, J. Exp. Theor. Phys. **70**, 1128 (1990).

[14] L.A. Reichertz, H. Dutz, S. Goertz, D. Krämer, W. Meyer, G. Reicherz, W. Thiel, and A. Thomas, Nucl. Instrum. Methods Phys. Res. A **340**, 278 (1994).

[15] P. Bösinger, E. Brun, and D. Meier, Phys. Rev. Lett. **38**, 602 (1977).

[16] P. Bösinger, E. Brun, and D. Meier, Phys. Rev. A **18**, 671 (1978).

[17] V.I. Yukalov and E.P. Yukalova, Phys. Rev. Lett. **88**, 257601 (2002).

[18] V.I. Yukalov, Laser Phys. **12**, 1089 (2002).

[19] V.I. Yukalov, Laser Phys. Lett. **2**, 356 (2005).

[20] A.V. Andreev, V.I. Emelyanov, and Y.A. Ilinsky, *Cooperative Effects in Optics* (Institute of Physics, Bristol, 1993).

[21] L. Mandel and E. Wolf, *Optical Coherence and Quantum Optics* (Cambridge University, Cambridge, 1995).

[22] P. Mataloni, E.De Angelis, and F. De Martini, Phys. Rev. Lett. **85**, 1420 (2000).

[23] E.De Angelis, F. De Martini, P. Mataloni, and M. Giangrasso, Phys. Rev. A **64**, 023809 (2001).

[24] V.I. Yukalov and E.P. Yukalova, Laser Phys. Lett. **2**, 302 (2005).

[25] V.I. Yukalov, Phys. Rev. B **71**, 184432 (2005).

[26] E. Ikonen, P. Helistö, T. Katila, and K. Riski, Phys. Rev. A **32**, 2298 (1985).

[27] E. Ikonen, P. Helistö, J. Hietaniemi, and T. Katila, Phys. Rev. Lett. **60**, 643 (1988).

[28] E. Ikonen, J. Hietaniemi, and T. Katila, Phys. Rev. B **38**, 6380 (1988).

[29] P. Helistö, I. Tittonen, M. Lippmaa, and T. Katila, Phys. Rev. Lett. **66**, 2037 (1991).

[30] T.M. Shavishvili, K.O. Khutsishvili, N.P. Fokina, and G.V. Lavrentiev, Tech. Phys. Lett. **15**, 33 (1989).

[31] N.P. Fokina and K.O. Khutsishvili, Phys. Met. Mallogr. **69**, 65 (1990).

[32] O.V. Nazarova, N.P. Fokina, and K.O. Khutsishvili, Phys. Met. Mallogr. **70**, 44 (1991).

[33] V.I. Yukalov, Phys. Rev. Lett. **75**, 3000 (1995).

[34] V.I. Yukalov, Phys. Rev. B **53**, 9232 (1996).

[35] V.I. Yukalov, Laser Phys. **2**, 559 (1992).

[36] N.P. Fokina, K.O. Khutsishvili, and S.G. Chkhaidze, J. Exp. Theor. Phys. **102**, 1013 (1992).

[37] K.O. Khutsishvili and S.G. Chkhaidze, Physica B **176**, 54 (1992).

[38] N.P. Fokina, K.O. Khutsishvili, and S.G. Chkhaidze, Physica B **179**, 171 (1992).

[39] V.I. Yukalov, Laser Phys. **5**, 970 (1995).

[40] T.S. Belozerova, V.K. Henner, and V.I. Yukalov, Laser Phys. **2**, 545 (1992).

[41] T.S. Belozerova, V.K. Henner, and V.I. Yukalov, Phys. Rev. B **46**, 682 (1992).

[42] T.S. Belozerova, C.L. Davis, and V.K. Henner, Phys. Rev. B **58**, 3111 (1998).

[43] O. Kahn, *Molecular Magnetism* (VCH, New York, 1993).

[44] B. Barbara, L. Thomas, F. Lionti, I. Chiorescu, and A. Sulpice, J. Magn. Magn. Mater. **200**, 167 (1999).

[45] A. Caneschi, D. Gatteschi, S. Sangregorio, R. Sessoli, L. Sorace, A. Cornia, M. Novak, C. Paulsen, and W. Wersendorfer, J. Magn. Magn. Mater. **200**, 182 (1999).

[46] A, Morello, F.L. Mettes, F. Luis, J.F. Fernandez, J. Krzystek, G. Aromi, G. Christou, and L.J. de Jongh, Phys. Rev. Lett. **90**, 017206 (2003).

[47] J. Villain, F. Hartmann-Boutron, R. Sessoli, and A. Rettori, Europhys. Lett. **27**, 159 (1994).

[48] P. Politi, A. Rettori, F. Hartmann-Boutron, and J. Villain, Phys. Rev. Lett. **75**, 537 (1995).

[49] V.I. Yukalov and E.P. Yukalova, Europhys. Lett. **70**, 306 (2005).

[50] C. Paulsen, J.G. Park, B. Barbara, R. Sessoli, and A. Canseschi, J. Magn. Magn. Mater. **140**, 379 (1995).

[51] F. Lionti, L. Thomas, R. Ballou, B. Barbara, A. Sulpice, R. Sessoli, and D. Gatteschi, J. Appl. Phys. **81**, 4608 (1997).

[52] H. De Raedt, S. Miyashita, K. Saito, D. Garcia-Pablos, and N. Garcia, Phys. Rev. B **56**, 11761 (1997).

[53] J.A. Perenboom, J.S. Brooks, S. Hill, T. Hathaway, and N.S. Dalal, Phys. Rev. B **58**, 330 (1998).

[54] W. Wersndorfer and R. Sessoli, Science **284**, 5411 (1999).

[55] W. Wernsdorfer, R. Sessoli, A. Caneschi, D. Gatteschi, A. Cornia, and D. Maily, J. Appl. Phys. **87**, 5481 (2000).

[56] E. Rastelli and A. Tassi, Phys. Rev. B **64**, 064410 (2001).

[57] E. Rastelli and A. Tassi, Phys. Rev. B **65**, 092413 (2002).

[58] K. Saito, S. Miyashita, and H. De Raedt, Phys. Rev. B **60**, 14553 (1999).

[59] M. Bal, J.R. Friedman, K. Mertes, W. Chen, E.M. Rumberger, D.N. Hendrickson, N. Avraham, Y. Myasoedov, H. Shtrikman, and E. Zeldov, Phys. Rev. B **70**, 140403 (2004).

[60] M. Motokawa, Rep. Prog. Phys. **67**, 1995 (2004).

Figure Captions

Fig. 1. Reduced spin variable s, for a cubic lattice, characterizing the spin polarization along the z-axis, as a function of dimensionless time (measured in units of T_2) for the Zeeman frequencies $\omega_0 = 1000$ (solid line), $\omega_0 = 2000$ (long-dashed line), and $\omega_0 = 5000$ (short-dashed line). The simulation is done for the molecules of spin $S = 10$, with the reduced initial polarization $s_0 = 0.9$. The anisotropy frequency is $\omega_D = 20$ and the resonator damping is $\gamma = 10$.

Fig. 2. Reduced spin polarization s, as a function of dimensionless time, for a cubic lattice, with $\omega_0 = 2000$ and $\omega_D = 20$, for the resonator damping $\gamma = 1$ (solid line), $\gamma = 10$ (long-dashed line), and $\gamma = 50$ (short-dashed line). The sample of molecules with spin $S = 10$ has the initial polarization $s_0 = 0.9$.

Fig. 3 Reduced spin polarization s, as a function of dimensionless time, for a cubic lattice, with $\omega_0 = 2000$, $\omega_D = 20$, $\gamma = 10$, $S = 10$, for different initial polarizations $s_0 = 0.9$ (solid line), $s_0 = 0.7$ (long-dashed line), and $s_0 = 0.5$ (short-dashed line).

Fig. 4 Spin polarization s, as a function of dimensionless time, for a cubic lattice, with $\omega_0 = 2000$, $\gamma = 10$, $S = 10$, and for different magnetic anisotropy values characterized by the anisotropy frequency $\omega_D = 20$ (solid line), $\omega_D = 50$ (long-dashed line), $\omega_D = 100$ (short-dashed line).

Fig. 5. Spin polarization s, as a function of dimensionless time, for a cubic lattice, with $\omega_0 = 2000$, $\omega_D = 20$, $\gamma = 10$, and $S = 10$, for two different cases, when the dipole interactions are present (solid line) and when they are absent (dashed line).

Fig. 6. Spin polarization s, as a function of dimensionless time, for a cubic lattice, with $\omega_0 = 2000$, $\omega_D = 20$, $\gamma = 1$, and for different spins $S = 10$ (solid line) and $S = 1/2$ (dashed line).

Fig. 7. Difference in the behavior of spin relaxation for different sample shapes and orientations, under the same values $\omega_0 = 2000$, $\omega_D = 20$, $\gamma = 30$, $S = 10$. The chain of spins along the z-axis (solid line); the chain of spins along the x-axis (long-dashed line); the plain of spins in the $y - z$ plane (short-dashed line), and the plane of spins in the $x - y$ plane (dashed-dotted line).
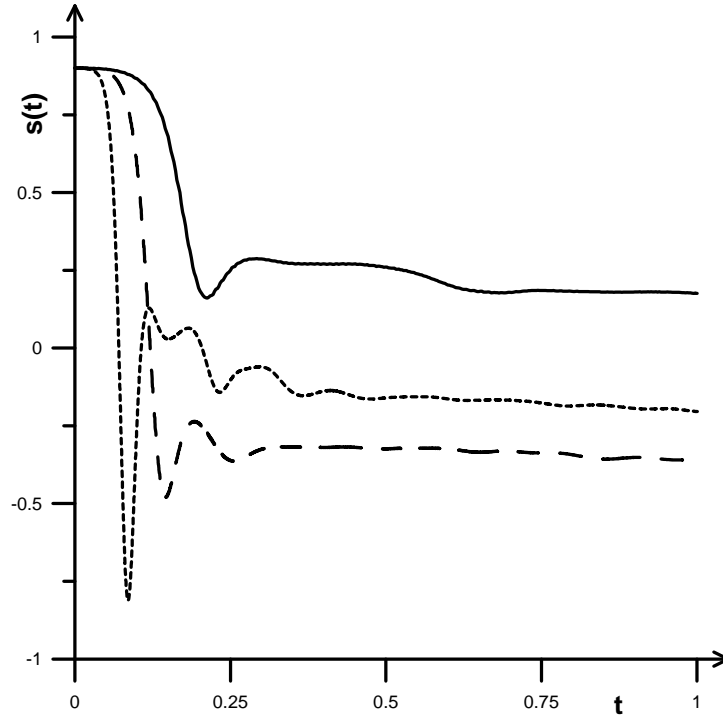
Figure 1: Reduced spin variable s, for a cubic lattice, characterizing the spin polarization along the z-axis, as a function of dimensionless time (measured in units of T_2) for the Zeeman frequencies $\omega_0 = 1000$ (solid line), $\omega_0 = 2000$ (long-dashed line), and $\omega_0 = 5000$ (short-dashed line). The simulation is done for the molecules of spin $S = 10$, with the reduced initial polarization $s_0 = 0.9$. The anisotropy frequency is $\omega_D = 20$ and the resonator damping is $\gamma = 10$.
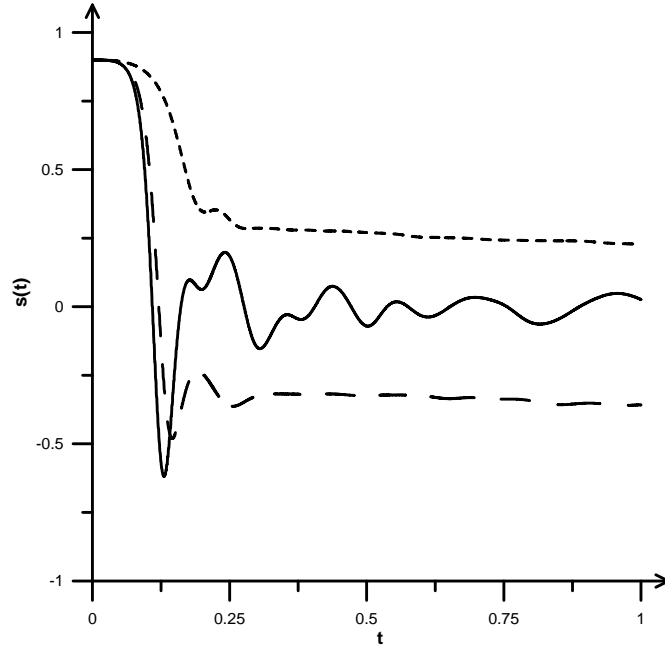
Figure 2: Reduced spin polarization s, as a function of dimensionless time, for a cubic lattice, with $\omega_0 = 2000$ and $\omega_D = 20$, for the resonator damping $\gamma = 1$ (solid line), $\gamma = 10$ (long-dashed line), and $\gamma = 50$ (short-dashed line). The sample of molecules with spin $S = 10$ has the initial polarization $s_0 = 0.9$.
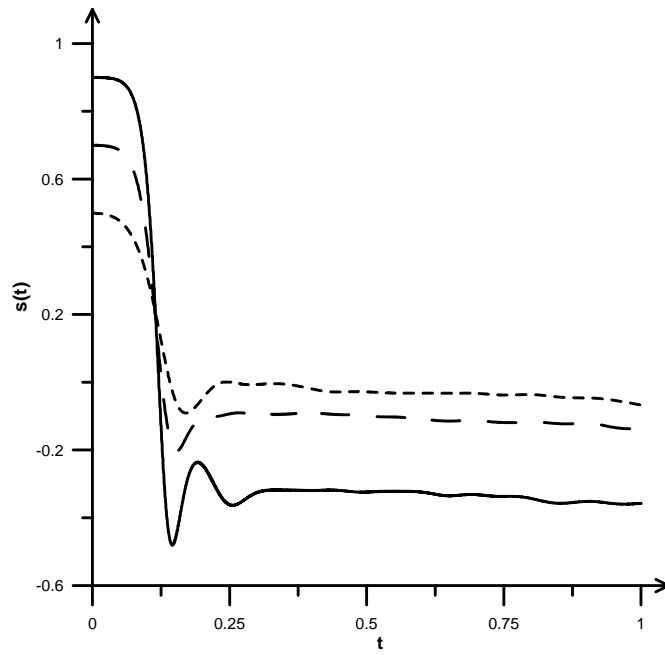
Figure 3: Reduced spin polarization s, as a function of dimensionless time, for a cubic lattice, with $\omega_0 = 2000$, $\omega_D = 20$, $\gamma = 10$, $S = 10$, for different initial polarizations $s_0 = 0.9$ (solid line), $s_0 = 0.7$ (long-dashed line), and $s_0 = 0.5$ (short-dashed line).
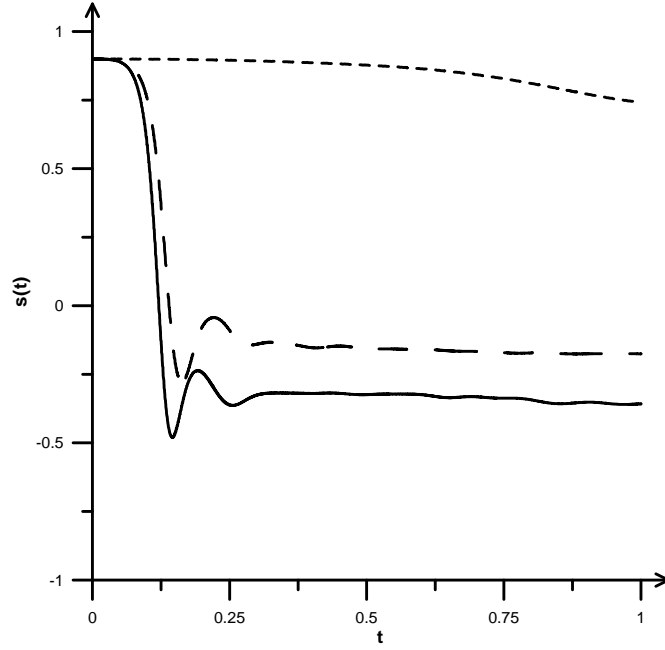
Figure 4: Spin polarization s, as a function of dimensionless time, for a cubic lattice, with $\omega_0 = 2000$, $\gamma = 10$, $S = 10$, and for different magnetic anisotropy values characterized by the anisotropy frequency $\omega_D = 20$ (solid line), $\omega_D = 50$ (long-dashed line), $\omega_D = 100$ (short-dashed line).
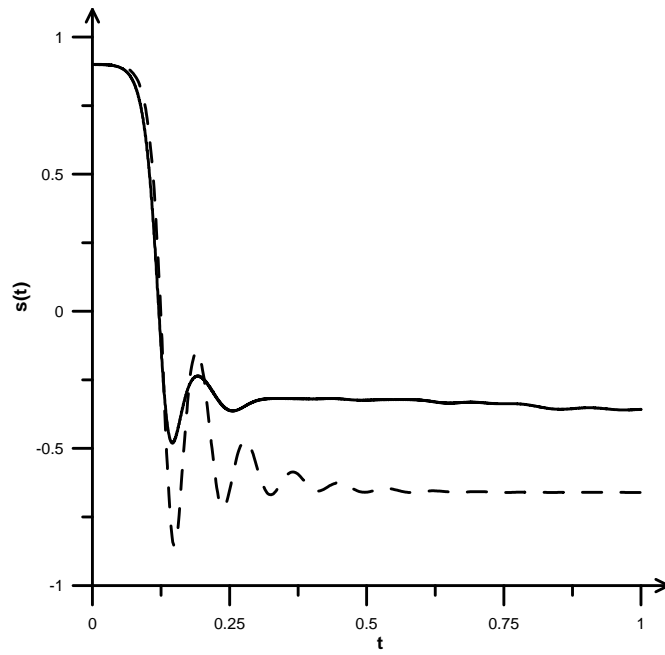
Figure 5: Spin polarization s, as a function of dimensionless time, for a cubic lattice, with $\omega_0 = 2000$, $\omega_D = 20$, $\gamma = 10$, and $S = 10$, for two different cases, when the dipole interactions are present (solid line) and when they are absent (dashed line).
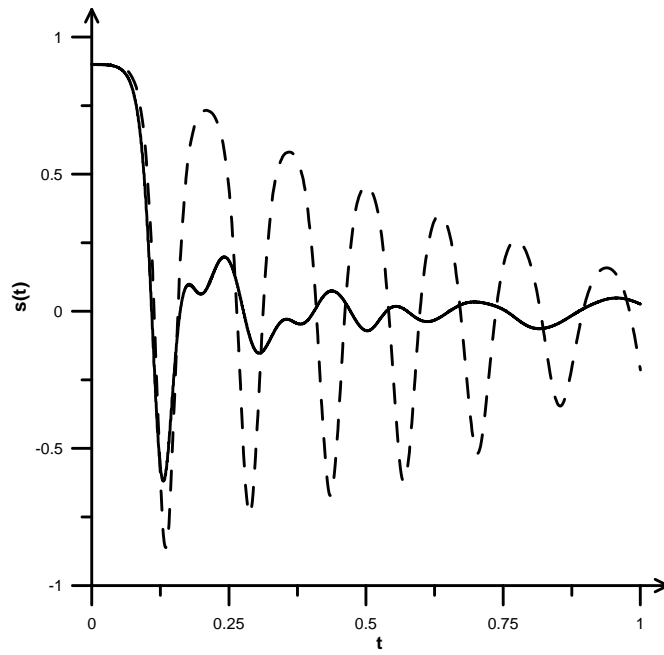
Figure 6: Spin polarization s, as a function of dimensionless time, for a cubic lattice, with $\omega_0 = 2000$, $\omega_D = 20$, $\gamma = 1$, and for different spins $S = 10$ (solid line) and $S = 1/2$ (dashed line).
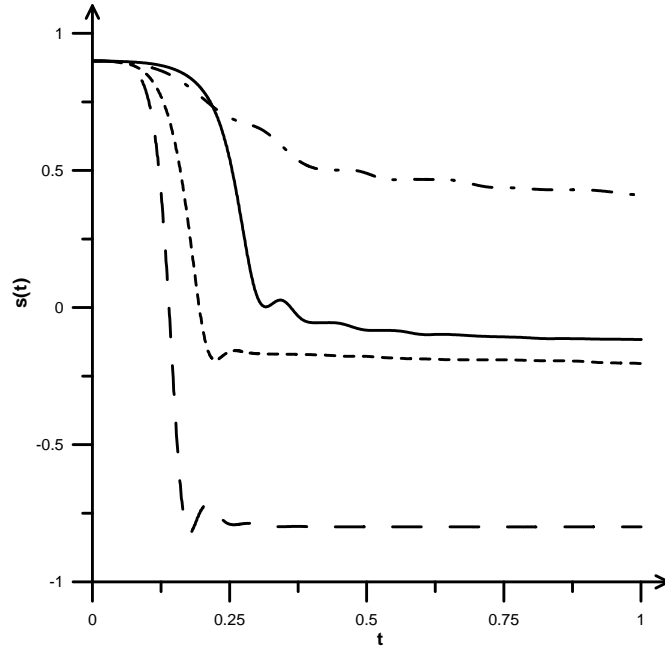
Figure 7: Difference in the behavior of spin relaxation for different sample shapes and orientations, under the same values $\omega_0 = 2000$, $\omega_D = 20$, $\gamma = 30$, $S = 10$. The chain of spins along the z-axis (solid line); the chain of spins along the x-axis (long-dashed line); the plain of spins in the $y - z$ plane (short-dashed line), and the plane of spins in the $x - y$ plane (dashed-dotted line).